DOI: 10.1002/cssc.200700165

Microporous Niobia–Silica Membrane with Very Low CO_2 Permeability

Vittorio Boffa,[a, c] Johan E. ten Elshof,*[a] Andrei V. Petukhov,[b] and Dave H. A. Blank[a]

A sol–gel-derived microporous ceramic membrane with an exceptionally low permeability for CO_2 from gaseous streams was developed and characterized. The sols were prepared from a mixture of niobium and silicon alkoxide precursors by acid-catalyzed synthesis. Microporous films were formed by coating asymmetric γ-alumina disks with the polymeric sol (Si/Nb = 3:1), followed by calcination at 500 °C. The membrane consists of a 150-nm-thick layer with a Si/Nb atomic ratio of about 1.5. The single-gas permeance of small gas molecules such as H_2, CH_4, N_2, and SF_6 decreases steadily with kinetic diameter. Hydrogen, helium, and carbon dioxide follow an activated transport mechanism through the membrane. The permeance of CO_2 in this membrane is much lower than that in pure silica, and its behavior deviates strongly from the general trend observed with the other gases. This is attributed to a relatively strong interaction between CO_2 and adsorption sites in the niobia–silica membrane.

Introduction

The increasing concern about climate change and the international agreements with demands for the reduction of CO_2 emissions[1] stress the importance of technologies that would enable the separation of CO_2 from gaseous streams. These technologies are important for the treatment of post-combustion gases in power plants,[2] exploitation of traditional gas resources[3] such as oil and natural gas fields, the development of renewable energy sources, for example, biogases,[4] and the gradual transition towards the so-called hydrogen economy.[5] The separation of CO_2 from gases containing hydrogen or hydrocarbons is usually done by physical adsorption, chemical reaction, cryogenic recovery, or a membrane process.[6] Absorption is currently the most common approach.

Membrane separation is also promising, because it can be applied to continuous processes and is energy efficient. Porous metal oxide membranes with pore sizes of less than 0.5 nm have been used for such molecular separations. The membranes have a high thermal and chemical stability and a high permeability to small gas molecules like hydrogen and water.[7] Both mesoporous (pore diameter 2–50 nm)[8] and microporous (pore diameter < 2 nm)[8] ceramic membranes can be used for CO_2 separation,[9,10] and the use of chemically modified mesoporous membranes was also demonstrated recently.[11] However, the highest separation selectivities have been obtained in the microporous regime, where the width of the pores is comparable to the molecular size of the permeating species. Microporous silica membranes are extremely effective molecular sieves. The permeability of gases in microporous silica decreases strongly with kinetic diameter.[12] However, the direct separation of a specific molecule like CO_2, with a kinetic diameter of 0.33 nm,[13] from a mixture containing both larger and smaller gases such as H_2 (0.28 nm), CH_4 (0.38 nm), CO (0.38 nm), N_2 (0.36 nm), and O_2 (0.35 nm) is only possible when differences in chemical properties between these gases are exploited to achieve separation.[13]

Here we report a new type of microporous ceramic membrane with a very low permeance for CO_2. Its separation performance is based on a combination of size-based sieving and variations in molecule–wall interactions between different types of gas molecules. We introduced active surface sites in the thin film to which carbon dioxide binds.[10] The active sites are probably pentavalent niobium ions in a microporous silicon oxide matrix. The membrane was made by sol–gel synthesis from a sol containing silicon and niobium alkoxide. The size of the sol particles was precisely controlled to enable the formation of a microporous material without mesopores or defects.

Results and Discussion

Sols were prepared from tetraethyl orthosilicate (TEOS) and niobium(V) penta(*n*-butyloxide) in an acidic alcoholic solution. As metal alkoxides derived from silicon are less sensitive to hydrolysis than those derived from niobium, TEOS was prehydrolyzed before reaction with $Nb^V(OC_4H_{11})_5$ (see Experimental Section). This type of sol is further referred to as NS sol, and the corresponding type of membrane is referred to as NS membrane.

[a] *Dr. V. Boffa, Dr. J. E. ten Elshof, Prof. D. H. A. Blank*
MESA+ Institute for Nanotechnology, University of Twente
P.O. Box 217, 7500 AE Enschede (The Netherlands)
Fax: (+31) 534893595
E-mail: j.e.tenelshof@utwente.nl

[b] *Dr. A. V. Petukhov*
Van't Hoff Laboratory for Physical and Colloid Chemistry
Debye Research Institute, Utrecht University
Padualaan 8, 3584 CH Utrecht (The Netherlands)

[c] *Dr. V. Boffa*
Present address: Dipartimento di Chimica Generale e Chimica Organica
Università di Torino, Corso M. D'Azeglio 48, 10125 Torino (Italy)

We studied the sol–gel synthesis of the niobia–silica mixed sol in detail so as to deposit layers of sufficient quality and suitable thickness. A diameter of 3–4 nm for the sol particles is sufficient to prevent penetration into the 5–8 nm wide pores of the underlying γ-alumina membrane support. Acid-catalyzed sol–gel synthesis leads to the formation of polymeric sols, which are not dense bodies but macromolecular chains formed by alternating metal and oxygen atoms. These macromolecules can be linear or branched. Mostly they are fractalic in nature and their shape can be characterized in terms of a fractal dimension D_f. The mass of such objects, M, scales with their size R according to Equation (1).[14]

$$M \propto R^{D_f} \quad (1)$$

The size and fractal dimension of the NS sol were determined by small-angle X-ray scattering (SAXS) using synchrotron radiation at the BM-26B station of the Dutch–Belgian beam line (DUBBLE) of the European Synchrotron Radiation Facility (Grenoble, France). SAXS allows estimation of the effective particle size and fractal dimension in solution. Figure 1a shows the raw SAXS data acquired by the gas-filled 2D detector; the position of the incident beam is indicated by an arrow. After background subtraction, the scattered intensity $I(q)$ was plotted as a function of the scattering vector q [nm^{-1}] in a Porod plot (Figure 1b) and a Guinier plot (Figure 1c). The scattering vector q is defined in Equation (2), where θ is the scattering angle and λ is the wavelength of the beam ($\lambda =$ 0.10 nm).[15] At small values of q, the scattering curve of a sol is related to the radius of gyration R_g of the particles through the Guinier law[15] [Eq. (3)].

$$q = \frac{2\pi}{\lambda}\sin(2\theta) \quad (2)$$

$$I(q) \propto \exp\left(-q^2\frac{R_g^2}{3}\right) \quad (3)$$

In Figure 1c, the logarithm of $I(q)$ varies approximately linearly with q^2. This allowed us to estimate the gyration radius of the NS particles by fitting the data in the range $0.16 \leq q \leq 0.35$ nm^{-1}. The best fit yielded a value of (3.3 ± 0.1) nm for R_g. This is of similar magnitude as that reported by Nair et al. for acid-catalyzed TEOS-derived silica sols.[16]

The fractal dimension D_f is also an important parameter and should be controlled to obtain a material with micropores only. A microporous network can only be formed when the sol particles can interpenetrate each other during film formation. Brinker and Scherer suggested that microporous silica can only be formed from sols with a D_f value of about 1.5 at the highest.[17]

The Porod plot shown in Figure 1b represents a scattering curve typical of polymeric metal-oxide sols.[16] The section of the curve between $q = 0.55$ nm^{-1} and $q = 2.09$ nm^{-1} is linear. This implies that $I(q)$ is a power function of q[15] [Eq. (4)]. We estimated the fractal dimension of the NS sol particles from Figure 1b by linear fitting, which yielded a D_f value of approximately 1.5. This suggests that the NS sol has a suitable size and polymeric shape for the preparation of a microporous thin film.

$$I(q) \propto q^{-D_f} \quad (4)$$

Membranes were prepared by dip-coating the NS sols on mesoporous γ-alumina asymmetric supports according to a procedure that has been described elsewhere.[18] Figure 2 shows a scanning electron microscopy (SEM) image of the cross-section of a membrane after calcination at 500 °C. The asymmetric architecture of the membrane is clearly visible. The thickness of the NS top layer was 150 nm.

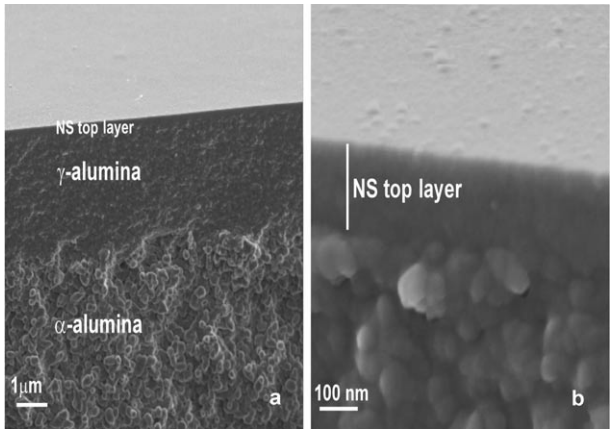

Figure 2. SEM images of the cross-section of an NS membrane: a) asymmetric three-layer structure, and b) magnified view of the 150-nm-thick NS top layer.

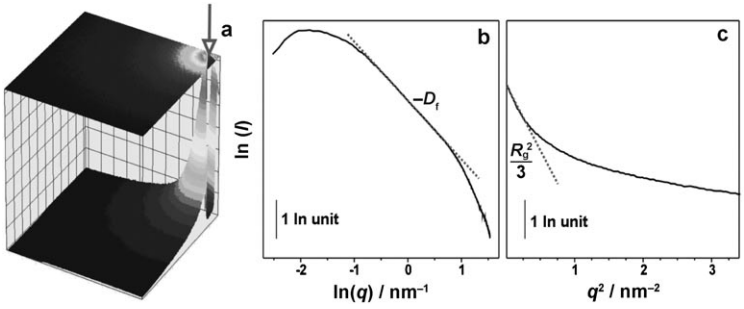

Figure 1. SAXS analysis of the NS sol. a) Raw data acquired from the 2D gas-filled detector of DUBBLE. The position of the incident beam is indicated by an arrow. After subtraction of the background and mask, the 1D data were plotted as a log–log plot (b) and as a Guinier plot (c). In both graphs, the intensity $I(q)$ is expressed in arbitrary units.

The compositions of the NS sol and the supported thin films were determined by X-ray fluorescence (XFR) and X-ray photoelectron spectroscopy (XPS), respectively. The atomic Si/Nb ratio of a dried NS sol was found to be 2.9. This is close to the atomic ratio of 3.0, in which the two metal precursors had been added. No other metals were detected by XRF measurements.

Figure 3 shows the atomic concentrations of Si, Nb, Al, and O as determined by XPS as a function of depth below the membrane surface. A 25- to 30-nm-thick transition region between the NS top layer and γ-alumina intermediate layer can

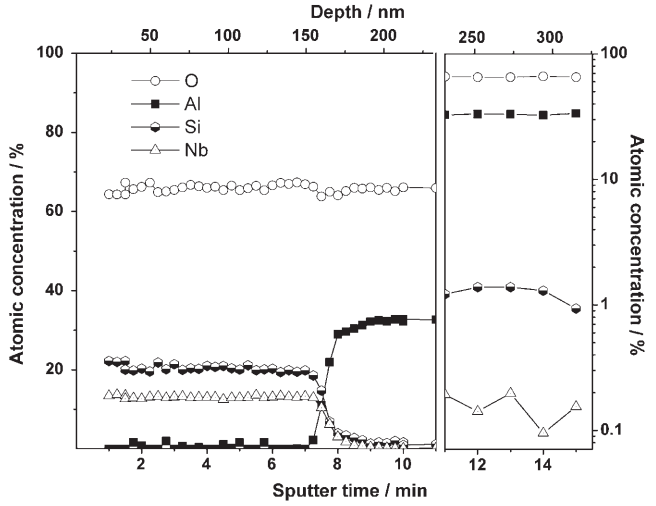

Figure 3. XPS depth profile of the NS membrane (Ar^+ sputtering rate 21 nm min^{-1}).

be observed at a depth of 150 nm. The Si/Nb ratio in the top layer is about 1.5. This is much lower than in the coating sol and may be explained by the higher reactivity of niobium alkoxides compared to TEOS. Niobium alkoxides condense faster than TEOS-based precursors, and this should eventually lead to a sol in which the larger particles have the higher niobium concentrations. At an estimated depth of about 250–300 nm, the atomic concentration of silicon is about 1 at%, while niobium traces up to about 0.1 at% were also detected. Hence, the Si/Nb molar ratio is about 10, that is, much higher than that in the original sol: This suggests that part of the TEOS in the sol did not react or reacted only to form small complexes or clusters. These clusters may have been drained into the support together with the solvent by capillary force as the coating procedure was carried out. As the extent to which the niobium precursor had already undergone hydrolysis and condensation was probably higher than for TEOS, Nb-rich sols were hardly drained into the support.

The permeances of a series of probe molecules with different masses and kinetic diameters were measured at 200 °C. The pressure difference across the membrane was 4 bar (Figure 4). The permeances of different gases before and after deposition of the NS layer are compared in Figure 4a, where the drawn line was obtained by fitting the expression for the flux, J_{Knud}, of a species in the Knudsen regime, under which condition most mesoporous membranes operate[19] [Eq. (5)] (ΔP is the difference between the partial pressures of the permeating species on the two sides of the membrane, L is the membrane thickness, M is the molecular mass of the permeating species, T refers to the absolute temperature, R is the gas constant, and K is a constant that depends on pore size and shape).

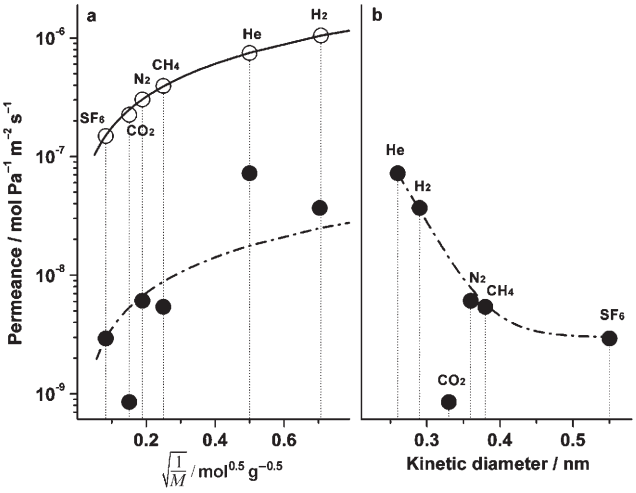

Figure 4. Single-gas permeation experiments: a) Knudsen plot of support and NS membrane. The Knudsen behavior of the support is indicated by the solid line, which was obtained by fitting experimental values to Equation (5). The prediction of Knudsen diffusion of the NS membrane is indicated by the dashed line, which was obtained by fitting to the experimental SF_6 permeance. b) Permeance as a function of kinetic diameter; the dashed line serves as a guide to the eye to indicate the approximate effect of size-sieving of the membrane.

$$J_{Knud} = K\sqrt{\frac{1}{MRT}}\frac{\Delta P}{L} \quad (5)$$

The agreement between the experimental data on the support and the Knudsen equation indicate a regime that is fully governed by transport through mesopores. The dashed line in Figure 4a was calculated from the experimental SF_6 permeance using Equation (5). Clearly, after addition of the NS layer the permeance of the membrane is no longer of the Knudsen type. A much better correlation was found between permeance and kinetic diameter, as indicated by the dashed line in Figure 4b. Except for CO_2, all probe molecules interact only weakly with the surface of the pores of the mixed metal oxide film, so that differences in permeance are primarily a result of size differences. The low permeance of nitrogen (kinetic diameter 0.36 nm) in the NS membrane suggests that a large fraction of the pores has a diameter that is smaller than that of nitrogen. However, the non-negligible permeance of the membrane to the largest gas molecule SF_6 (kinetic diameter 0.55 nm) reveals the presence of a small fraction of pores or defects larger than 0.55 nm.

The permeance of CO_2 was exceptionally low considering its moderate molecular size. A roughly six times higher permeance would be expected based on the behavior of the other probes. At 200 °C, the ideal separation factor for CO_2/SF_6 mixture is 0.29 instead of the value of 1.8 predicted by the Knudsen mechanism. This indicates that the transport of SF_6 occurs through large micropores. If transport would take place primarily through mesopores or defects, the permeance of CO_2 should be equal to or larger than the permeance of SF_6.

The permeances of He, H_2, and CO_2 in the NS top layer versus temperature are shown in Figure 5. Molecular transport in micropores occurs essentially according to a thermally acti-

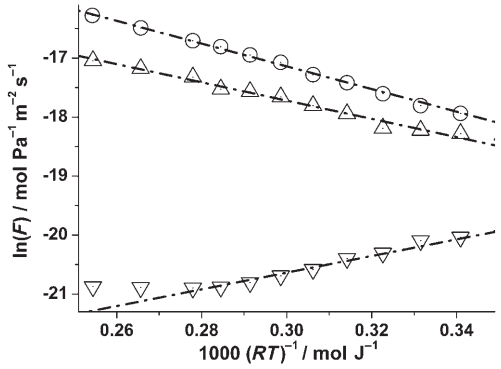

Figure 5. Arrhenius plots of the permeance (F) of He, H_2, and CO_2 in the NS top layer.

vated diffusion mechanism, which can be expressed in terms of a modified Fick law[20] [Eq. (6)] (J_0 is a temperature-independent coefficient, and E_a is the apparent activation energy and the sum of two contributions: the heat of sorption of the molecule (a negative number, as adsorption is an exothermic process) and the activation energy of mobility).

$$J = J_0 \exp\left(-\frac{E_a}{RT}\right)\frac{\Delta P}{L} \qquad (6)$$

As these two terms have opposite signs, the apparent activation energy can be positive or negative, depending on their relative magnitudes. A negative value of E_a is generally interpreted as being caused by strong adsorption of the molecule on the pore surface. Table 1 lists the activation energies calculated from Figure 5, together with some data on pure and metal-oxide-doped silica membranes that have been reported elsewhere.[20–26] The values measured in the present study are close to those reported by Nair et al., who found activation energies for helium permeance of 23 kJ mol^{-1} in silica.[21] Asaeda and co-workers reported an increase in apparent activation energy of H_2 permeance from 3.4 to 44 kJ mol^{-1} when the Zr dopant loading in silica was increased from 10 mol% to 90 mol%.[26]

The apparent activation energy of CO_2 was calculated by a linear fit of all data points below 150 °C. This yielded a value of (−14.2 ± 0.8) kJ mol^{-1}. Such a highly negative value suggests a high enthalpy of sorption. The literature values in Table 1 indicate either positive activation energies for CO_2 permeance[22,23] or slightly negative values.[20] Apart from data in a study in which activation energies of −9.2 to −11.2 kJ mol^{-1} were measured,[24] none of the reported values is close to (−14.2 ± 0.6) kJ mol^{-1} as measured on the NS membrane.

Figure 6 compares the H_2/CO_2 and CH_4/CO_2 ideal permselectivities of the NS membrane at different temperatures with that of the support. The ideal permselectivity of the support

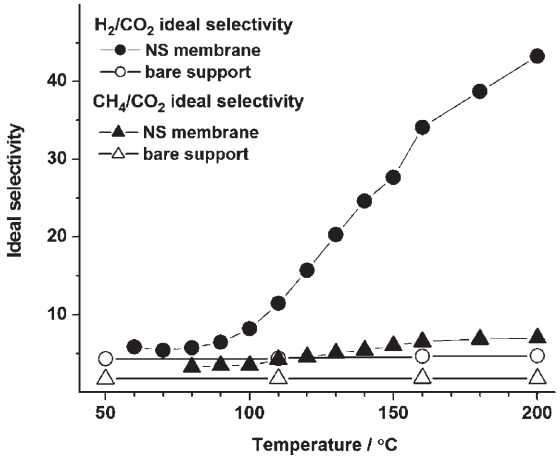

Figure 6. Ideal permselectivities of H_2/CO_2 (circles) and CH_4/CO_2 (triangles) as calculated from single-gas permeation experiments in the temperature range 50–200 °C. Filled symbols refer to the NS membrane; unfilled symbols refer to the bare support.

Table 1. Apparent activation energies (E_a) for molecular transport of He, H_2, and CO_2 in NS top layer.[a]

Sample	E_a [kJ mol^{-1}]			T_{anneal}	Ref.
	He	H_2	CO_2	[°C]	
NS	19.1 ± 0.3	15.3 ± 0.7	−14.2 ± 0.8	500	–
SiO_2	–	7.6	−4	400	[20]
SiO_2	–	8	−2	600	[20]
SiO_2	7 ; 23	–	–	400	[21]
SiO_2		12.3; 21.7	3; 6.8	400	[22]
SiO_2	4; 9	10; 11	0; 10	400	[23]
SiO_2	1.7; 4.0	−1.3; 2.9	−9.2; −11.2	360–570	[24]
33% Ni/SiO_2	7.1	–	–	500	[25]
10% ZrO_2/SiO_2	4.7	3.4	–	570	[26]
50% ZrO_2/SiO_2	22	44	–	570	[26]

[a] Calculated by fitting the data reported in Figure 5. Also shown is their comparison with literature values for pure and doped silica membranes prepared by sol-gel coating. Membrane annealing temperatures are also reported. When more values were presented in a single study, the lowest one is reported on the left side of the semicolon and the highest one is shown on the right side.

for both mixtures was approximately temperature-independent and close to the theoretical limits predicted by the Knudsen law, that is, roughly equal to the square root of the ratio of molecular masses of the two species. On the other hand, the permselectivity of the NS membrane towards H_2/CO_2 increased rapidly as a function of temperature. This is probably a result of the high activation energy of mobility of hydrogen and the large heat of sorption of carbon dioxide. The ideal H_2/CO_2 selectivity was 5.8 at 60 °C and increased to 43.2 at 200 °C. A similar but less prominent trend was observed for CH_4/CO_2. The ideal selectivity increased from 3.3 at 80 °C to 7.0 at 200 °C. These measurements indicate that NS could be a suitable membrane material for CO_2 sequestration from streams containing hydrogen and/or methane.

We attempted to investigate the absorption of CO_2 onto the surface of NS pores in more detail by employing IR spectroscopy. We first studied CO_2 adsorption on a powder that was obtained by calcining dried NS sol using the same heating pro-

gram as for the NS membrane. However, we obtained a black powder with extremely low surface area (as revealed by nitrogen sorption analysis) after calcination, and IR sorption measurements of sufficient quality on these samples were not possible.

Adsorption of CO_2 was therefore measured by attenuated total reflectance Fourier transform infrared (ATR/FTIR) spectroscopy on a 94-nm-thick NS film that was spin-coated on a ZnSe crystal and calcined at 250 °C. A 126-nm-thick film of pure silica was used as a reference. The thickness of the films was determined by XPS including depth-profiling as discussed above. Figure 7 shows the IR spectra of the two samples. The

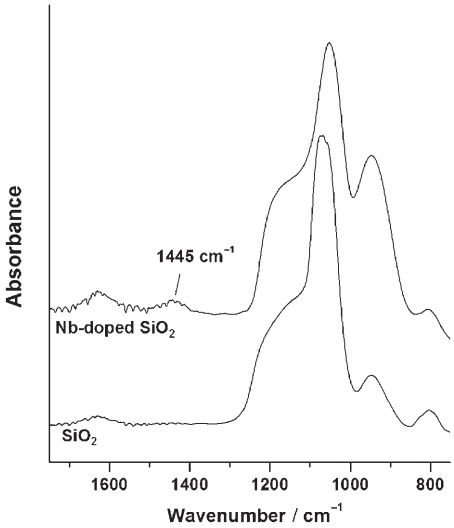

Figure 7. Room-temperature ATR/FTIR spectra of pure silica and NS films in nitrogen atmosphere.

vibrations of the SiO_4^{4-} tetrahedron[27] in both samples are visible at 804–806 and 1050–1070 cm^{-1}. The high-intensity peak in the NS sample at a wavenumber of 948 cm^{-1} is attributed to niobium atoms in the oxide network.[27] Although the same peak is visible in the spectrum of silica, its intensity is markedly higher when some niobia is also present. A sorption band at 1445 cm^{-1} is visible in the spectrum of niobium-doped silica. This band is commonly assigned to carbonate-like species on the surface of the metal oxide.[28,29] As expected, this peak was absent in the spectrum of silica. Surface carbonates are strongly bound species and presumably do not play a determining role in the transport rate of CO_2 at 200 °C.[30–31] The band at 1445 cm^{-1} is too broad to enable determination of specific types of carbonates.

In a second series of experiments, the measuring cell was flushed with CO_2 at a rate of 10 mL min^{-1}. The IR absorption spectrum was recorded as function of time. Only the part of the spectrum between 2280 and 2400 cm^{-1} changed upon exposure to CO_2. This can be attributed to changes in stretching mode vibrations of CO_2 in the gas phase and adsorbed CO_2. Figure 8 shows the temporal evolution of the band. A comparison is made with the spectrum of pure CO_2 as measured on a bare ZnSe crystal, that is, without significant contribution of

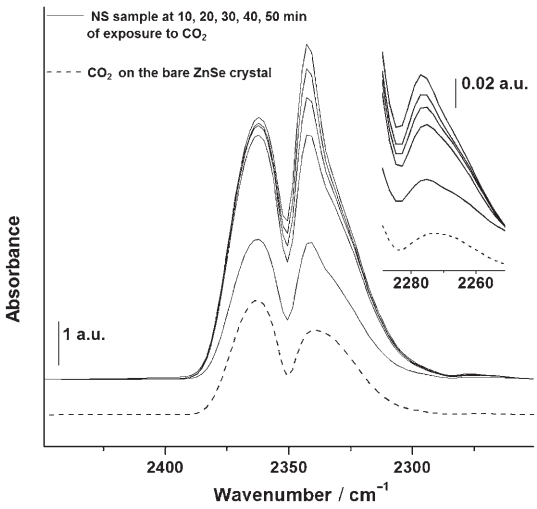

Figure 8. Asymmetric stretch (ν_3) region of the room-temperature ATR/FTIR spectra of CO_2 adsorbed on NS (solid lines) and CO_2 measured on a bare ZnSe crystal (dashed line). The inset shows a magnified view of the $^{13}CO_2$ ν_3 asymmetric stretch region.

adsorbed CO_2. The intensity of the band increased with time, but even after 50 min a steady-state value had not been reached. This is probably due to the fact that the pores of the material are so narrow that the crossover of CO_2 diffusing into the micropores and N_2 diffusing out of the micropores is rate-determining. The band at 2345 cm^{-1} is not present in the spectrum of gaseous CO_2 and agrees well with data on CO_2 adsorption on silicalite.[30–32] It has been ascribed to a ν_3 stretching vibration of CO_2 sorbed on surface cations.[29–32] A further indication for CO_2–wall interactions is provided by the band related to characteristic $^{13}CO_2$ ν_3 asymmetric stretching mode (see inset, Figure 8). This band has an intensity that is about 100 times lower than that of the corresponding $^{12}CO_2$ signal depicted in the main body of the figure. Its position is at 2277 cm^{-1} for NS and at 2271 cm^{-1} for pure CO_2. The spectrum of CO_2 sorbed on the silica film showed a qualitatively similar evolution as on NS (data not shown). This suggests that CO_2 interacts with hydroxy groups on the pore wall in both silica and niobia-doped silica rather than with niobium ions exposed on the surface. The fact that the main band of the CO_2 stretching band is present at 2345 cm^{-1} in the spectra of both silica and NS is not in conflict with the data reported in Table 1. In fact, Pires et al.[32] observed similar CO_2 ν_3 stretching frequencies in zeolites, which displayed heats of CO_2 sorption that differed by more than 10 kJ mol^{-1}. We therefore propose that the low permeance of CO_2 in NS is primarily due to strong adsorption of CO_2 on surface hydroxy groups, presumably those which are directly bound to Nb. The more polar character of the Nb–OH bonds in NS will lead to a stronger interaction with CO_2 than surface OH groups that are connected to Si.

Conclusions

The microporous niobia–silica membrane represents a new type of gas-selective ceramic membrane with which it might

become possible to separate CO_2 from gas mixtures. Compared to state-of-the-art silica membranes,[12] the fluxes and selectivities exhibited by the newly developed NS membrane are much lower. The non-negligible flow of SF_6 is an indication that a small fraction of supermicropores is still present in the membrane. Further optimization of the preparation procedure should result in elimination of all pores larger than about 0.55 nm.

The exceptionally low permeance of CO_2 is explained as a consequence of strong chemical interaction between CO_2 and the pore surface of the microporous material, presumably Nb-bound hydroxy groups. The results reported here indicate that other microporous doped silica membranes might also be developed in order to design molecular separations based on sorption rather than on differences in molecular size between molecules.

Experimental Section

Synthesis of the NS membrane: Tetraethyl orthosilicate (11 mL; Aldrich, 99.999% pure) was added to ethanol (10.5 mL), and then an aqueous solution of nitric acid was dropped in the mixture to obtain the final molar ratio $OC_2H_5/H_2O/HNO_3 = 1:0.5:0.01$. We have chosen to express the chemical composition of the sol in this way because alkoxy groups, water, and acid are the moieties that participate directly in the reaction. This mixture was heated under reflux at 60 °C for 2 h. Then, a 1 M solution of niobium(V) penta(*n*-butyloxide) (Gelest) in *n*-butanol (Aldrich, anhydrous) was added slowly to the mixture. Aqueous nitric acid was dropped into the mixture to restore the initial composition $(M)OR/H_2O/HNO_3$ to 1:0.5:0.01 (M = Si, Nb; R = C_2H_5, C_4H_9). The sol was heated at reflux at 60 °C for 5 h and then cooled down to −20 °C and kept at this temperature for a few days until it was used for characterization or membrane preparation.

SAXS characterization: The sample was placed in a capillary glass tube (diameter 1.5 mm), which was exposed at room temperature to an X-ray beam (12 keV). The beam was focused on a corner of the 2D detector to maximize the range of accessible q values. By placing the 2D detector of DUBBLE at a distance of 1.5 m from the sample, it was possible to measure the scattered intensity in a range of q (scattering vector) values between 0.10 and 5.20 nm^{-1} with successive steps of 0.01 nm^{-1}. A beam stop was required to shield the detector from the direct beam and thus to avoid saturation of the outgoing signal (the position of the beam stop is marked by a triangular shadow in Figure 1a). The raw data was corrected for the pixel-dependent detector sensitivity and averaged along circles with the same q values. To correct for the background contribution, a SAXS curve of a capillary containing pure solvent was recorded under the same experimental conditions as the NS sol.

Membrane preparation: The NS membrane was prepared by dipping a porous support into the NS sol. The porous support consisted of a 2-mm-thick α-alumina disk, coated on one side with a 6% La-doped γ-alumina film of about 2-μm thickness. The NS coating was deposited on the γ-alumina layer, which had an average pore diameter of about 4 nm. This was done in a class 1000 clean room using an automatic dip-coating machine, with an angular dipping rate of 0.06 rad s^{-1}. The membrane was calcined in air at 500 °C, using heating and cooling rates of 0.5 °C min^{-1}.

Characterization of membrane morphology: The thicknesses and morphologies of the NS membranes were analyzed by scanning electron microscopy (SEM) on a LEO 1550 FEG. X-ray photoelectron spectroscopy (XPS) measurements were performed on a PHI Quantera Scanning ESCA microprobe equipped with a monochromatic AlKα X-ray source (1486.6 eV) at a pressure of less than 8×10^{-6} bar. Film thickness was determined by monitoring the atomic composition of the film at different depths after sputtering the material with Ar^+ ions. The sputter rate was calibrated using a 100-nm SiO_2 film on silicon. The chemical composition of a powdered sample of the NS sol was measured by X-ray fluorescence (XRF) using a Philips PW1480 apparatus.

Gas permeation experiments: Single-gas permeation measurements were performed in a dead-end mode setup. Permeabilities of gases with different kinetic diameter were measured at 5 bar at the feed side and atmospheric pressure at the retentate side. The gas flow was measured with a soap film flow meter. As atmospheric water can condense in the pores of the silica matrix, all membranes were dried at 200 °C in a hydrogen flow for at least 16 h before any measurements were made. The permeation rates of different gases were determined in a sequence starting with the gas with the smallest kinetic diameter, and equilibrating for a few hours each time that a new gas was introduced into the setup. The Arrhenius plots were obtained by varying the membrane temperature from 200 °C to 50 °C. The resistance of the support for H_2, He, CO_2, and CH_4 was measured at 200, 160, 110, and 50 °C. The resistance at other temperatures was obtained by fitting these data to Equation (5).

ATR measurements: A thin film of niobium-doped silica was prepared by spin-coating the NS sol on a ZnSe crystal. The ZnSe crystal was completely covered by the NS sol and spun for 20 s at a speed of 2000 rpm. This procedure was repeated five times. Then, the thin film was dried at 250 °C for 3 h (heating/cooling rates of 0.5 °C min^{-1}). As a reference, a thin film of silica was prepared following the same protocol using a standard polymeric silica sol.[20] The ATR measurements were performed at room temperature on a Bruker Tensor 27 equipped with a MCT detector in a dedicated measuring cell, which is described elsewhere.[33] The total volume of the cell was 120 μL. The samples were first exposed to nitrogen for about 1 h and then to a continuous flow of CO_2 (10 mL min^{-1}) at a pressure of 1 bar.

Acknowledgements

Financial support from the Netherlands Technology Foundation (STW) is gratefully acknowledged. The authors would like to thank Dr. H. L. Castricum and Dr. Riaan Schmuhl (University of Twente) for their help in the SAXS experiment and contributions to the analysis, J. A. P. Gelten and Dr. B. Mojet (University of Twente) for their assistance in the ATR/FTIR experiments, and G. Magnacca and P. Cerrato (Università di Torino) for useful discussions. We are grateful to the Dutch Organization for the Scientific Research (NWO) for giving us beam time to perform SAXS measurements at DUBBLE, and to Florian Meneau, Wim Bras, and Dirk Detollenaere (DUBBLE beam line) for onsite assistance.

Keywords: adsorption · carbon dioxide · membranes · niobium · silicon

[1] United Nations Framework on Climate Change (UNFCCC), *The Kyoto Protocol to the Convention on Climate Change*, **1997**, available at http://unfccc.int/resource/docs/convkp/kpeng.pdf.
[2] O. Bolland, P. Mathieu, *Energy Convers. Manage.* **1998**, *39*, 1653–1663.
[3] B. D. Bhide, S. A. Stern, *J. Membr. Sci.* **1993**, *81*, 209–237.
[4] M. Röhr, R. Wimmerstedt, *Desalination* **1990**, *77*, 331–345.
[5] D. R. Simbeck, *Energy* **2004**, *29*, 1633–1641.
[6] R. Bredesen, K. Jordal, O. Bolland, *Chem. Eng. Process.* **2004**, *43*, 1129–1158.
[7] M. Mulder, *Basic Principles of Membrane Technology*, Kluwer Academic, Dordrecht, **1996**, p. 59.
[8] K. S. W. Sing, D. H. Everett, R. A. W. Haul, L. Moscou, R. A. Pierotti, J. Rouquerol, T. Siemieniewska, *Pure Appl. Chem.* **1985**, *57*, 603–619.
[9] R. J. R. Uhlhorn, K. Keizer, R. J. van Vuren, A. J. Burggraaf, *J. Membr. Sci.* **1989**, *39*, 285–300.
[10] R. J. R. Uhlhorn, K. Keizer, A. J. Burggraaf, *J. Membr. Sci.* **1989**, *46*, 225–241.
[11] B. A. McCool, W. J. DeSisto, *Adv. Funct. Mater.* **2005**, *15*, 1635–1640.
[12] R. M. de Vos, H. Verweij, *Science* **1998**, *279*, 1710–1711.
[13] D. W. Breck, *Zeolite Molecular Sieves—Structure, Chemistry, and Use*, John Wiley & Sons, New York, **1974**, p. 636.
[14] B. B. Mandelbrot, *The Fractal Geometry of Nature*, W. H. Freeman. New York, **1982**, p. 123.
[15] R. J. Roe, *Methods of X-ray and Neutron Scattering in Polymer Science*, Oxford University Press, New York, **2000**.
[16] N. B. Nair, W. J. Elferink, K. Keizer, H. Verweij, *J. Colloid Interface Sci.* **1996**, *178*, 565–570.
[17] C. J. Brinker, G. W. Scherer, *Sol-Gel Science*, Harcourt Brace Jovanovich, Boston, **1990**, p. 779.
[18] A. Nijmeijer, H. Kruidhof, R. Bredesen, H. Verweij, *J. Am. Ceram Soc.* **2001**, *84*, 136–140.
[19] R. R. Bhave, *Inorganic Membranes: Synthesis, Characteristics and Applications*, Van Nostrand Reinhold, New York, **1991**, p. 338.
[20] R. M. de Vos, H. Verweij, *J. Membr. Sci.* **1998**, *143–157*, 37.
[21] B. N. Nair, K. Keizer, H. Suematsu, Y. Suma, N. Kaneko, S. Ono, T. Okubo, S.-I. Nakao, *Langmuir* **2000**, *16*, 4558–4562.
[22] R. S. A. de Lange, K. Keizer, A. J. Burggraaf, *J. Membr. Sci.* **1995**, *104*, 81–100.
[23] R. J. R. Uhlhorn, K. Keizer, A. J. Burggraaf, *J. Membr. Sci.* **1992**, *66*, 271–287.
[24] T. Yoshioka, E. Nakanishi, T. Tsuru, M. Asaeda, *AIChE J.* **2001**, *47*, 2052–2063.
[25] M. Kanezashi, T. Fujita, M. Asaeda, *Sep. Sci. Technol.* **2005**, *40*, 225–238.
[26] K. Yoshida, Y. Hirano, H. Fujii, T. Tsuru, M. Asaeda, *J. Chem. Eng. Jpn.* **2001**, *34*, 523–530.
[27] Y. Liu, K. Murata, M. Inaba, *Chem. Lett.* **2003**, *32*, 992–993.
[28] A. A. Davydov, *Infrared Spectroscopy of Adsorbed Species on the Surface of Transition Metal Oxides*, John Wiley & Sons, West Sussex, **1984**.
[29] M. Cerruti, C. Morterra, *Langmuir* **2004**, *20*, 6382–6388.
[30] B. Bonelli, B. Onida, B. Fubini, C. Otero Areán, E. Garrone, *J. Phys. Chem. B* **2000**, *104*, 10978–10988.
[31] B. Bonelli, B. Onida, B. Fubini, C. Otero Areán, E. Garrone, *Langmuir* **2000**, *16*, 4976–4983.
[32] J. Pires, M. Brotas de Carvalho, F. Ramôa Ribeiro, E. G. Derouane, *J. Mol. Catal.* **1993**, *83*, 295–303.
[33] S. D. Ebbesen, B. L. Mojet, L. Lefferts, *Langmuir* **2006**, *22*, 1079–1085.

Received: December 20, 2007
Published online on April 15, 2008

